Journal of Theoretical and Applied Mechanics, Sofia, Vol.51 (2021) pp. 22-34
SOLID MECHANICS

EVALUATION OF THE MACROMECHANICAL PROPERTIES OF PLA-BASED NANOCOMPOSITES BY MEANS OF THREE-POINT BENDING METHOD

TODOR BATAKLIEV*

OLEM, Institute of Mechanics, Bulgarian Academy of Sciences, Acad. G. Bonchev St., Bl. 4, Sofia 1113, Bulgaria

[Received: 04 January 2020. Accepted: 30 April 2020]

ABSTRACT: The synergistic effect of using two carbon nanofillers in PLA die on the nanocomposites mechanical properties was studied in the present work. The polylactic acid is relatively brittle and semi-crystalline polymer selected to be used as matrix because of its biodegradable features. It was modified with graphene nanoplatelets (GNP) and multiwall carbon nanotubes (MWCNT) by means of melt extrusion preparation method. The maximum flexural stress and tangent modulus of elasticity of 3D printed nanocomposite samples were defined by three-point bending experiments using UMT-2 equipment. It was found that some compounds, incorporated with both graphene and carbon nanotubes in the PLA structure, exhibit better mechanical performance comparing to the nanocomposites loaded with single carbon nanofiller. SEM analysis was made to assess the carbon fillers dispersion.

KEY WORDS: polylactic acid, composites, synergism, three-point bending, SEM analysis.

1 INTRODUCTION

Three-point bending analysis represents nowadays one of the main techniques for macromechanical characterization of wide range of materials as polymer-based nanocomposites, porous metal oxide films, epoxy resin, ceramics or heterogeneous structural materials [1–5]. The method consists of crosshead motion of a loading nose onto the flatwise sample operating at constant force rates. Considering composites loaded with graphene or other carbon material the three-point bending appears to be a really valuable tool for the evaluation of flexural modulus and elastic modulus enhancement upon incorporation of the filler [6].

Polymer matrix composites suggest high flexural strength and elasticity [7]. Moreover, they are relatively more susceptible for precise uniform manufacturing of complex preshaped products [8]. Recently, the polylactic acid-based composites are widely studied and used because of their mechanical and biodegradable properties

*Corresponding author e-mail: todorbat@gmail.com

[9,10]. Considerably features' enhancement can be obtained by reinforcing the polymer with relatively small amounts of nanomaterials, which are nanosized at least in one dimension [11]. It have been found that the graphene sheets consist of wrinkled structures and in between the wrinkles there are sections having surface roughness of $\sim$ 4–5 Å. This surface roughness could present a preferential nucleation site for crystalline phases when graphene is dispersed in a polymer matrix [12]. That potential change of polymer's crystallinity can have impact on the mechanical properties of the composite.

Three point bending test method has been used to study the effect of nanoclay addition into epoxy matrix on the mechanical properties of hybrid carbon/fiberglass composites [13], fatigue properties of carbon fiber epoxy matrix composite laminates [14], flexural strength and modulus of hybrid green composites [15] and flexural strength profile of PLA composites with cellulose and bronze as additives [16]. The impact of polycaprolactone (PCL) and silicon carbide (SiC) contents on the flexural properties and fracture toughness of PLA/PCL/SiC composites was investigated using three-point bending test configuration [17]. It has been found that the elastic modulus of PLA decreased after the introduction of PCL but increased after the addition of SiC whiskers.

In another article [18], the influence of aerographite thermal treatment on the mechanical performance of aerographite-epoxy nanocomposite by determining the fracture toughness in three-point bending tests has been investigated. The effect of GNPs on the flexural properties of HDPE-based nanocomposite was reported to be significant at 1 wt% graphene content [19]. The decline in flexural strength at 2 and 3 wt% GNPs loading has been explained with an additional stress accumulation mechanism caused by increasing of nanocomposite pores size as well as by aggregates formation of graphene particles in the in-plane level. The combination of high aspect ratio of CNTs and larger surface area of GNPs has an important contribution to the synergistic effect of nanofiller hybrids concerning the mechanical properties of epoxy composites [20].

The current literature on instrumented mechanical testing provides apparently conflicting information on the synergistic effect of polymer nanocomposites as regards the mechanical properties. Moreover, there is a lack of research papers dedicated to mechanical properties assignation of PLA-based composites modified with carbon nanofillers by using three-point bending technique. Bending damage commonly occurs when the nanocomposite components are used for different engineering applications. However, the knowledge on the bending properties of polymer nanocomposites is still very limited. Therefore, in this paper, we report on the three-point bending properties of GNPs and MWCNTs reinforced PLA-based composite. This approach might be accepted as a novelty considering the chemical and physical

features of semi-crystalline hydrophilic polymer. In the present study, the synergistic effect of graphene nanoplatelets and multiwall carbon nanotubes on the mechanical properties enhancement of biodegradable polymer composites has been investigated by employing three-point bending test method.

2 Experimental

2.1 Materials

Ingeo^{TM}Biopolymer PLA-3D850 with MFR 7–9 g/10 min (210°C, 2.16 kg) was purchased from Nature Works. TNIGNP-Industrial Graphene nanoplatelets – average thickness < 30 nm and diameter of $\sim$ 5–7 μm; purity 90% and TNIMH4-OH functionalized MWCNTs (TNIMH): OD: 10–30 nm; Length: 10–30 μm; SSA = 110 m^2/g; EC > 100 S/cm; purity 95% were supplied from TimesNano, China.

2.2 Preparation and characterization methods

Monofiller (GNP/PLA and MWCNT/PLA) and bifiller (GNP/MWCNT/PLA) compounds have been made by means of melt extrusion technique. Some details regarding the fabrication of composites and filaments are described in previous publications [21, 22]. Strips with geometry $60 \times 12 \times 2.4$ mm, printing density of 100% and possessing very low roughness were prepared by 3D printing using filament with diameter of 1.75 mm and applying FDM technique and layer-to-layer deposition. The set of samples was made with German RepRap X-400 Pro 3D printer having two printing heads and equipped with Simplify3D slicer. The specimens were laid down in flat build orientation under nozzle temperature of 210°C, layer thickness of 0.25 mm and printing speed of 2600 mm/min. All samples were held in a vacuum package or in desiccator in order to protect them from air humidity. The composites analyzed by three-point bending are listed in Table 1.

The morphology of the PLA-based nanocomposites was observed by a scanning electron microscope (SEM, SH 4000M, Hirox, USA). 3D printed samples were immersed in liquid nitrogen, then cut to get visibility of the inner layers in cross-section surface and finally coated with gold (layer thickness ˜200) using a sputter coater (Q150RS plus, Quorum, USA).

Three-point bending tests were made on UMT-2 Universal Tester (modular system) developed by Bruker. All experiments were performed with 1–100 kg (1000 N) force sensor utilizing a three-point loading system applied to a simply supported 3D printed sample. The essential parameters as maximum flexural stress and tangent modulus of elasticity (or bending Young's modulus) were defined according to ASTM standard test methods (D 790–07) for flexural properties of unreinforced and reinforced plastics, including high-modulus composites in the form of rectangular

Table 1: List of composites tested by three-point bending technique

No	Sample index	PLA content (wt%)	MWCNT content (wt%)	GNP content (wt%)
1	PLA	100	—	—
2	3MWCNT	97	3	—
3	6MWCNT	94	6	—
4	9MWCNT	91	9	—
5	12MWCNT	88	12	—
6	3GNP	97	—	3
7	6GNP	94	—	6
8	9GNP	91	—	9
9	12GNP	88	—	12
10	1.5GNP1.5MWCNT	97	1.5	1.5
11	1.5GNP4.5MWCNT	94	4.5	1.5
12	3GNP3MWCNT	94	3	3
13	4.5GNP1.5MWCNT	94	1.5	4.5
14	3GNP6MWCNT	91	6	3
15	6GNP3MWCNT	91	3	6
16	3GNP9MWCNT	88	9	3
17	9GNP3MWCNT	88	3	9
18	6GNP6MWCNT	88	6	6

bars. Flexural strength cannot be determined for those materials that do not break or that do not fail in the outer surface of the test specimen within the 5.0% strain limit of these test methods. The sample is deflected until rupture occurs in the outer surface of the test specimen or until a maximum strain of 5.0% is reached, whichever occurs first. Midspan deflection and rate of crosshead carriage motion were calculated prior to each test and the relevant values were inserted in a script of the instrumental software, see Eq. (1) and (2).

$$R = \frac{ZL^2}{6d} \,, \tag{1}$$

where R is the rate of crosshead motion [mm/min], L is the support span [mm], d is the depth of beam [mm], and Z is the rate of straining of the outer fiber [mm/mm/min]. Z shall be equal to 0.01.

$$D = \frac{rL^2}{6d} \,, \tag{2}$$

where D is the midspan deflection [mm], r is the strain [mm/mm], L is the support span [mm], d is the depth of beam [mm].

The test should be terminated when the maximum strain in the outer surface of the test specimen has reached 0.05 mm/mm or at break if break occurs prior to reaching the maximum strain. The deflection at which this strain will occur may be calculated by letting r equal 0.05 mm/mm. For flat-wise tests the support span shall be 16 (tolerance ± 1) times the depth of the 3D printed strip. When a homogeneous elastic material is tested in flexure as a simple beam supported at two points and loaded at the midpoint, the maximum stress in the outer surface of the specimen occurs at the midpoint. This stress may be calculated for any point on the load-deflection curve by means of the following equation:

$$\sigma_f = \frac{3PL}{2bd^2} \,, \tag{3}$$

where σ_f is stress in the outer fibers at midpoint [MPa], P is load at a given point on the load-deflection curve [N], L is the support span [mm], b is width of beam [mm], d is the depth of beam [mm].

The tangent modulus of elasticity is the ratio, within the elastic limit, of stress to corresponding strain. It is calculated by drawing a tangent to the steepest initial

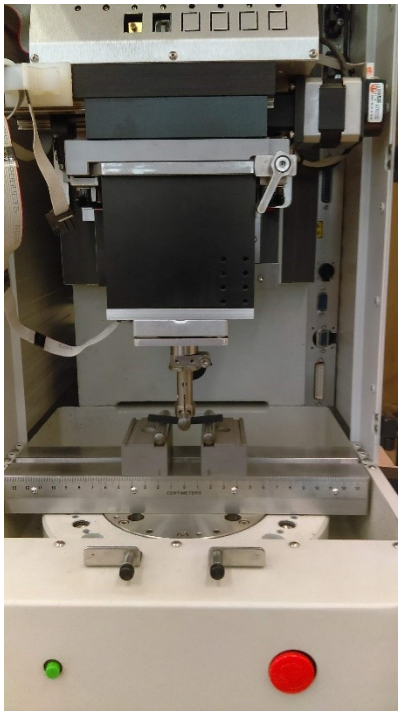

Fig. 1: Experimental set-up of three-point bending analysis using UMT-2 equipment.

straight-line portion of the load-deflection curve and using Eq. (4):

$$E_B = \frac{L^3 m}{4bd^3} \ , \tag{4}$$

where E_B is modulus of elasticity in bending [MPa], L is the support span [mm], b is width of beam [mm], d is the depth of beam [mm], m is slope of the tangent to the initial straight-line portion of the load-deflection curve [N/mm] of deflection.

A representative image of the experimental set-up during three-point bending test over PLA-based nanocomposite strip is shown in Fig.1.

3 Results and Discussion

3.1 Three-point bending analysis

The most important result of each one three-point bending test is the calculation of maximum flexural stress (MFS) and tangent modulus of elasticity (TME) of the material. These parameters are derived by the relevant stress-strain curve received after the experiment using the instrument software. The effect of 12 wt% carbon filler loading in PLA matrix on the stress-strain curves of the nanocomposites compared to the neat polymer is presented in Fig. 2. The slopes of σ–ε in the initial linear elastic regime are indicative regarding the obtained values of tangent modulus of elasticity

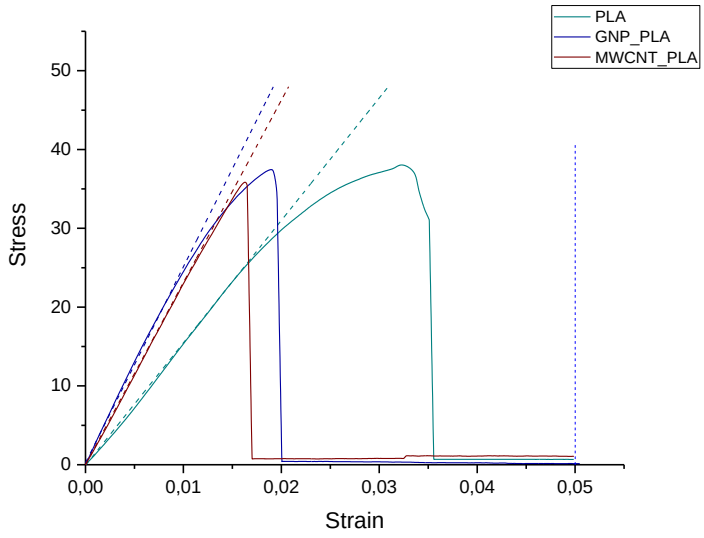

Fig. 2: Typical stress-strain curves showing different linear elastic portion and fracture point, respectively, for pure PLA, 12 wt% GNP/PLA and 12 wt% MWCNT/PLA nanocomposites.

whereas the stress level of fracture point defines the maximum flexural stress of the specimen.

It can be seen that the impact of carbon nanotubes on the curve describing the dependence of MFS on nanocomposite loading is greater than the influence of graphene nanoplatelets, especially at 3 wt% and 9 wt% MWCNTs loadings (Fig. 3a). This is due to the interfacial polymer-filler interaction related to the distinct hybrid structure between MWCNTs and polymer chains [23]. The registered slightly lower MFS

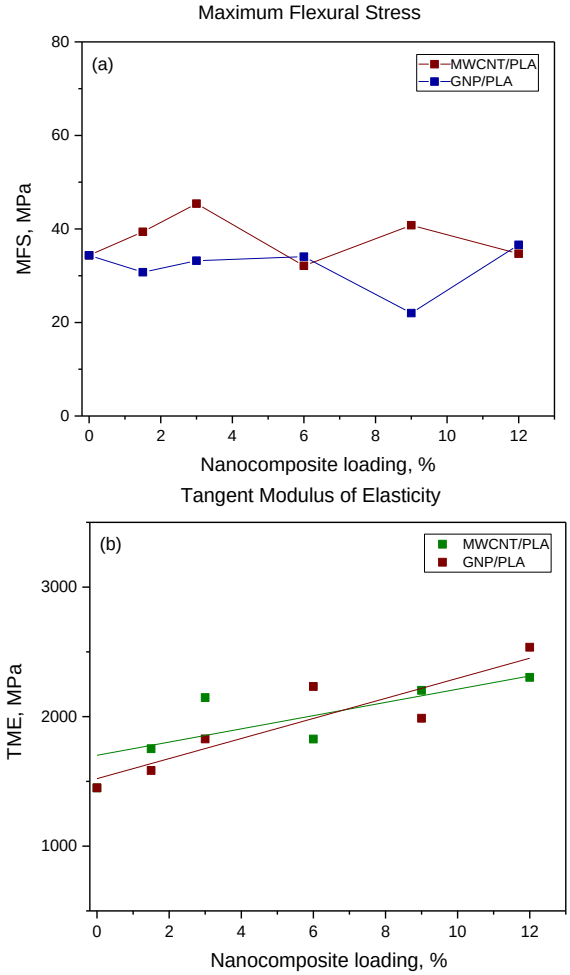

Fig. 3: Maximum flexural stress (a) and tangent modulus of elasticity (b) of PLA-based nanocomposites having single carbon filler in the hybrid structure.

value of the composite 9 wt% GNP/PLA was assigned to relatively poor filler dispersion fortunately not affecting the obtained tangent modulus of elasticity. The values of tangent modulus of elasticity (TME) are getting higher for both MWCNT/PLA and GNP/PLA nanocomposites with increasing carbon nanofiller loading (Fig. 3b). Nevertheless, the effect of graphene on that macromechanical feature of the composite is a bit more significant as 60% improvement of TME was registered with rising filler loading up to 12 wt% GNPs concentration. It should be mentioned the clearly noticeable elasticity of the samples modified with graphene nanoplatelets in the experimental running of bending process.

Among the nanocomposites having overall 3 wt% and 6 wt% carbon loading pre-

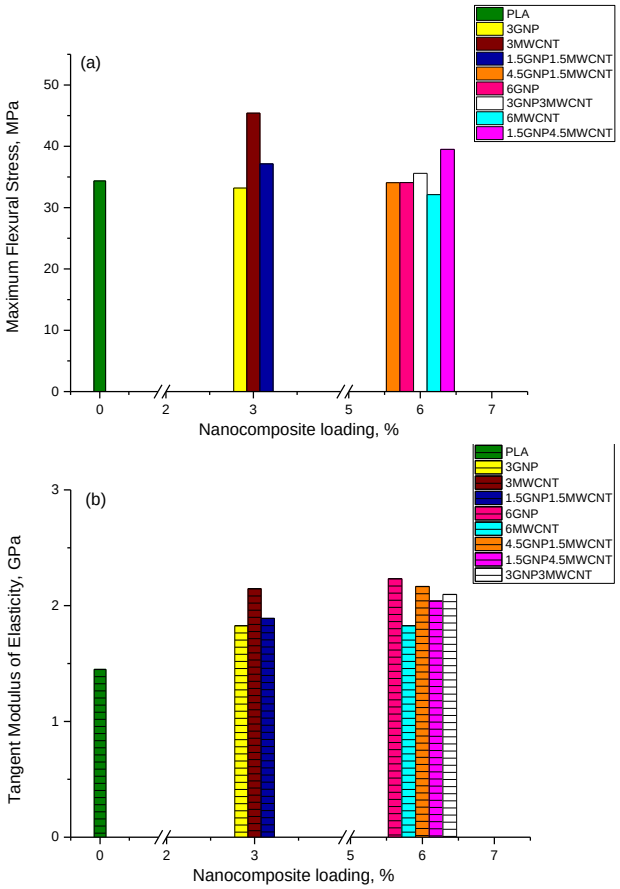

Fig. 4: Maximum flexural stress (a) and tangent modulus of elasticity (b) of GNP/MWCNT/PLA nanocomposites with overall 3 wt% and 6 wt% carbon loading.

sented in Fig. 4a it should be mentioned the higher MFS belonging to the samples with greater concentration of MWCNTs in PLA matrix as the monofiller compound 3 wt% MWCNT/PLA and the bifiller compound 1.5 wt% GNP/4.5 wt% MWCNT/PLA. The flexural properties of the latter are distinct evidence about the presence of synergistic effect of both carbon nanofillers incorporated in the polymer base. Maximum flexural stress improvement of the nanocomposites containing carbon nanotubes was not surprising in terms of the exceptional hardness possessed by that filler [24].

Better elasticity of the nanocomposites with rising graphene concentration can be seen in Fig. 4b reflecting in TME values above 2 GPa for the samples 6 wt% GNP/PLA and 4.5 wt% GNP/1.5 wt% MWCNT/PLA. Among the samples having

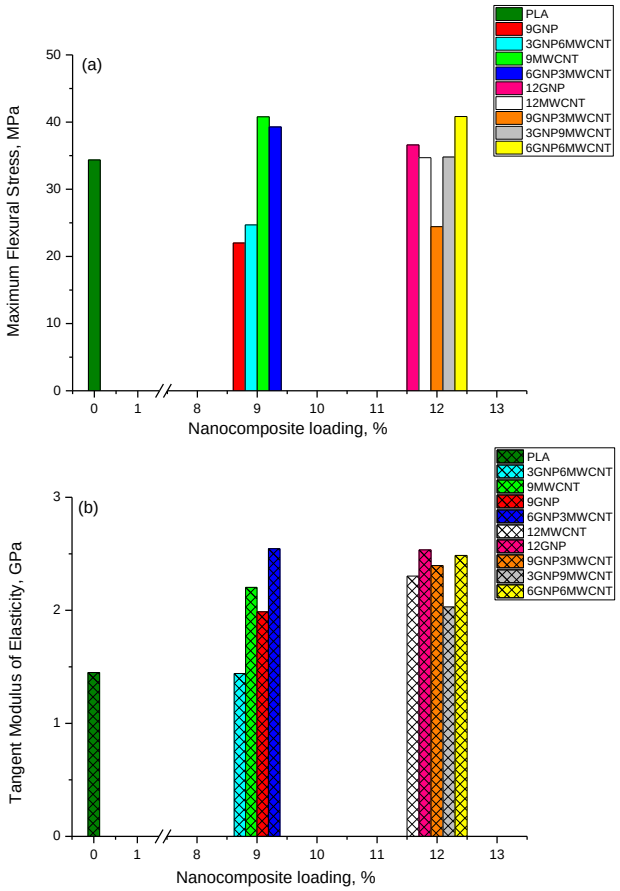

Fig. 5: Maximum flexural stress (a) and tangent modulus of elasticity (b) of GNP/MWCNT/PLA nanocomposites with overall 9 wt% and 12 wt% carbon loading.

3 wt% carbon filler content, the composite 3 wt% MWCNT/PLA showed significant macromechanical properties that might be due to excellent nanofiller dispersion. Two nanocomposites having 9 wt% carbon filler in PLA matrix demonstrated excellent flexural strength – 9 wt% MWCNT/PLA and 6 wt% GNP/3 wt% MWCNT/PLA, see Fig. 5a.

The noticed bifiller composite as well as the mixed compound 6 wt% GNP/6 wt% MWCNT/PLA possess sensibly higher modulus of elasticity compared to the pure polymer, as shown in Fig. 5b. The received comparatively low MFS and TME values concerning several nanocomposites as 9 wt% GNP/PLA and notably 3 wt% GNP/6 wt% MWCNT/PLA could be due to shear deflections related to worst carbon nanoparticles distribution that resulted in reduction of the apparent flexural properties. Exceptional modulus of elasticity can be seen for the nanocomposite 12 wt% GNP/PLA (Fig. 5b). This fact is anticipated outlining the graphene material reinforcement and can be consistent with the homogeneous carbon filler distribution in PLA matrix reached by melt extrusion technique.

3.2 Scanning Electron Microscopy analysis

SEM microscopy has been applied to do morphological characterization of carbon nanotubes inserted in polymer-based nanocomposites [25]. The micrographs presented in Fig. 6 were made by focusing the instrument over cross-section sample surface. The received SEM images of bifiller nanocomposites 3 wt% GNP/3 wt% MWCNT/PLA (Fig. 6a) and 6 wt% GNP/6 wt% MWCNT/PLA (Fig. 6b) revealed good uniform distribution of carbon nanoparticles within the PLA matrix. It can be seen that the combination of both nanofillers forms an interconnected network

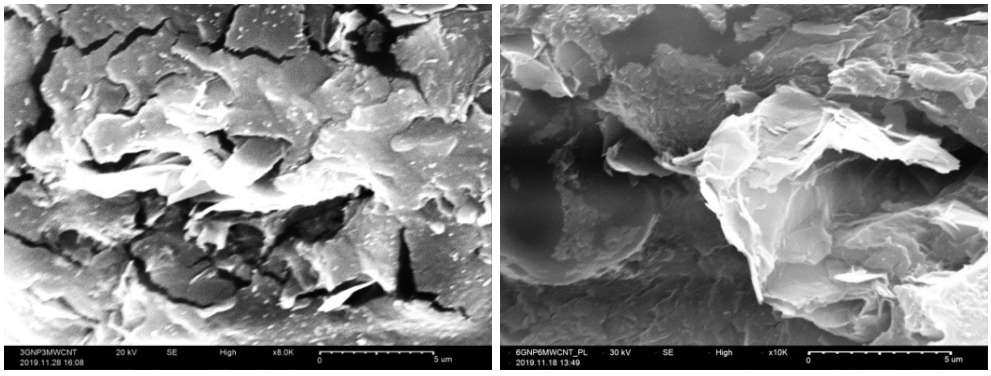

Fig. 6: SEM micrographs of 3 wt% GNP/3 wt% MWCNT/PLA (a) and 6 wt% GNP/6 wt% MWCNT/PLA (b) nanocomposites.

in the polymer matrix that leads to unique synergetic effect in the improvement of macromechanical properties of the as prepared nanocomposites.

4 Conclusions

Applying three-point bending as macromechanical method was met to disclose the synergistic effect of graphene and carbon nanotubes on the mechanical properties of PLA-based nanocomposites. Good carbon nanoparticles distribution in the polymer matrix was confirmed by SEM analysis of the composites having mixed GNPs and MWCNTs loading. Generally, the graphene filler improves the elastic properties of nanocomposites whereas the carbon nanotubes are responsible for higher rigidity of the compounds. Three-point bending analysis revealed distinct indications of synergism regarding the mixed nanocomposites 6 wt% GNP/3 wt% MWCNT/PLA and 6 wt% GNP/6 wt% MWCNT/PLA. This mechanical reinforcement of the nanocomposites is probably related to the structure and particle geometry of the hybrid fillers, the interactions between the fillers, the impact of carbon nanoparticles concentration and the processing method. According to melt extrusion process and evidenced by SEM analysis, the graphene and the carbon nanotubes seem to be highly dispersed in the composite structure.

Acknowledgments

This work was supported by the Grant No BG05M2OP001-1.002-0011, financed by the Science and Education for Smart Growth Operational Program (2014-2020) and co-financed by the European Union through the European structural and Investment funds.

This work has received funding from the European Union's Horizon 2020-MSCA-RISE-734164 Graphene 3D Project and by the H2020-FET-Graphene Flagship-881603 Graphene Core 3 Project. The author would like to acknowledge the contribution of the Bilateral collaboration between IMech, BAS and IPCB-CNR, Napoli/Portici (2019-2021).

References

[1] A.R. Torabi, A.S. Rahimi, M.R. Ayatollahi (2019) Elastic-plastic fracture assessment of CNT-reinforced epoxy/nanocomposite specimens weakened by U-shaped notches under mixed mode loading. *Composites Part B* **176** 107114.

[2] J.-H. Chen, W.-S. Luo (2017) Flexural Properties and Fracture Behavior of Nanoporous Alumina film by Three-Point Bending Test. *Micromachines* **8** 206.

[3] D. O'Brien, P.T. Mather, S.R. White (2001) Viscoelastic Properties of an Epoxy Resin during Cure. *Journal of Composite Materials* **35** 883-904.

[4] L. PRÖBSTER, U. MAIWALD, H. WEBER (1996) Three-point bending strength of ceramics fused to cast titanium. *European Journal of Oral Sciences* **104** 313-319.

[5] J. TONG, P. CHEN, J. ZHAO, B. ZHAO (2019) Fracture test of nanocomposite ceramics under ultrasonic vibration based on nonlocal theory. *Ceramics International* **45** 20945-20953.

[6] H. MALEK-MOHAMMADI, G.H. MAJZOOBI, J. PAYANDEHPEYMAN (2019) Mechanical Characterization of Polycarbonate Reinforced With Nanoclay and Graphene Oxide. *Polymer Composites* **40** 3947-3959.

[7] S.K. SINGH, A. KUMAR, A. JAIN (2018) Improving tensile and flexural properties of SiO_2-epoxy polymer nanocomposite. *Materials Today* **5** 6339-6344.

[8] M. MONIRUZZAMAN, K.I. WINEY (2006) Polymer Nanocomposites Containing Carbon Nanotubes. *Macromolecules* **39** 5194.

[9] B. FIEDLER, F. GOJNY, M.H.G. WICHMANN, M.C.M. NOLTE, K. SCHULTE (2006) Fundamental aspects of nano-reinforced composites. *Composites Science and Technology* **66** 3115-3125.

[10] F. HUSSAIN, M. HOJJATI, M. OKAMOTO, R.E. GORGA (2006) Review article: Polymer-matrix Nanocomposites, Processing, Manufacturing, and Application: An Overview. *Journal of Composite Materials* **40** 1511-1575.

[11] M. CADEK, J.N. COLEMAN, V. BARRON, K. HEDICKE, W.J. BLAU (2002) Morphological and mechanical properties of carbon-nanotube-reinforced semicrystalline and amorphous polymer composites. *Applied Physics Letters* **81** 5123.

[12] H.C. SCHNIEPP, J.L. LI, M.J. MCALLISTER, H. SAI, M. HERRERA-ALONSO, D.H. ADAMSON, R.K. PRUD'HOMME, R. CAR, D.A. SAVILLE, I.A. AKSAY (2006) Functionalized single graphene sheets derived from splitting graphite oxide. *Journal of Physical Chemistry B* **110** 8535-8539.

[13] G. ONER, H.Y. UNAL, Y. PEKBEY (2018) Mechanical Performance of Hybrid Carbon/Fiberglass Composite Laminates Reinforced with Nanoclay. *Acta Physica Polonica A* **134** 164-167.

[14] T. YANG, M. HE, X. NIU, Y. DU (2016) Experimental Investigation of the Three-point Bending Fatigue Properties of Carbon Fiber Composite Laminates. *Advances in Material Science* **1** 1-6.

[15] R.B. YUSOFF, H. TAKAGI, A.N. NAKAGAITO (2016) Tensile and flexural properties of polylactic acid-based hybrid green composites reinforced by kenaf, bamboo and coir fibers. *Industrial Crops and Products* **94** 562-573.

[16] K.G. JAYA CHRISTIYAN, U. CHANDRASEKHAR, K. VENKATESWARLU (2019) Investigation on the Mechanical Properties of PLA & Its Composite Fabricated Through Advanced Fusion Plastic Modelling. *Journal of Mechanical Engineering Research and Developments* **42** 47-54.

[17] J. CHEN, T.Y. ZHANG, F.L. JIN, S.J. PARK (2018) Fracture Toughness Improvement of Poly(lactic acid) Reinforced with Poly(ε-caprolactone) and Surface-Modified Silicon Carbide. *Advances in Materials Science and Engineering* Article ID 6537621.

[18] J. MARX, S. ROTH, A. BROUSCHKIN, D. SMAZNA, Y.K. MISHRA, K. SCHULTE, R. ADELUNG, B. FIEDLER (2019) Tailored crystalline width and wall thickness of an annealed 3D carbon foam composites and their mechanical properties. *Carbon* **142** 60-67.

[19] G.V. SERETIS, D.E. MANOLAKOS, C.G. PROVATIDIS (2018) On the graphene nanoplatelets reinforcement of extruded high density polyethylene. *Composites Part B: Engineering* **145** 81-89.

[20] S. CHATTERJEE, F. NAFEZAREFI, N.H. TAI, L. SCHLAGENHAUF, F.A. NESCH, B.T.T. CHU (2012) Size and synergy effects of nanofiller hybrids including graphene nanoplatelets and carbon nanotubes in mechanical properties of epoxy composites. *Carbon* **50** 5380-5386.

[21] E. IVANOV, R. KOTSILKOVA, X. HESHENG, Y. CHEN, R. DONATO, K. DONATO, A.P. GODOY, R. DI MAIO, C. SILVESTRE, S. CIMMINO, V. ANGELOV (2019) PLA/Graphene/MWCNT Composites with Improved Electrical and Thermal Properties Suitable for FDM 3D Printing Applications. *Applied Sciences* **9** 1209.

[22] R. KOTSILKOVA, P. ANGELOVA, T. BATAKLIEV, V. ANGELOV, R. DI MAIO, C. SILVESTRE (2019) Study on aging and recover of poly(lactic) acid composite films with graphene and carbon nanotubes produced by solution blending and extrusion. *Coatings* **9** 359.

[23] BATAKLIEV, T., I. PETROVA-DOYCHEVA, V. ANGELOV, V. GEORGIEV, E. IVANOV, R. KOTSILKOVA, M. CASA, C. CIRILLO, R. ADAMI, M. SARNO, P. CIAMBELLI (2019) Effects of Graphene Nanoplatelets and Multiwall Carbon Nanotubes on the Structure and Mechanical Properties of Poly(lactic acid) Composites: A Comparative Study. *Applied Sciences* **9** 469.

[24] B. PENG, M. LOCASCIO, P. ZAPOL, S. LI, S.L. MIELKE, G.C. SCHATZ, H.D. ESPINOSA (2008) Measurements of near-ultimate strength for multiwalled carbon nanotubes and irradiation-induced crosslinking improvements. *Nature Nanotechnology* **3** 626-631.

[25] Y.Z. KETEKLAHIJANI, M. ARJMAND, U. SUNDARARAJ (2017) Cobalt Catalyst Grown Carbon Nanotube/Poly(Vinylidene Fluoride) Nanocomposites: Effect of Synthesis Temperature on Morphology, Electrical Conductivity and Electromagnetic Interference Shielding. *ChemistrySelect* **2** 10271-10284.